

See discussions, stats, and author profiles for this publication at: <https://www.researchgate.net/publication/271591202>

Direct Observation of Interlayer Hybridization and Dirac Relativistic Carriers in Graphene/MoS₂ van der Waals Heterostructures

ARTICLE in NANO LETTERS · JANUARY 2015

Impact Factor: 13.59 · DOI: 10.1021/nl504167y · Source: PubMed

CITATIONS

5

READS

308

6 AUTHORS, INCLUDING:



J. Avila

SOLEIL synchrotron

159 PUBLICATIONS 2,323 CITATIONS

[SEE PROFILE](#)



Rafik Addou

University of Texas at Dallas

39 PUBLICATIONS 435 CITATIONS

[SEE PROFILE](#)



Maria Carmen Asensio

SOLEIL synchrotron

205 PUBLICATIONS 3,494 CITATIONS

[SEE PROFILE](#)



Matthias Batzill

University of South Florida

116 PUBLICATIONS 4,354 CITATIONS

[SEE PROFILE](#)

Direct Observation of Interlayer Hybridization and Dirac Relativistic Carriers in Graphene/MoS₂ van der Waals Heterostructures

Horacio Coy Diaz,[†] José Avila,[‡] Chaoyu Chen,[‡] Rafik Addou,[†] Maria C. Asensio,[‡] and Matthias Batzill*,[†]

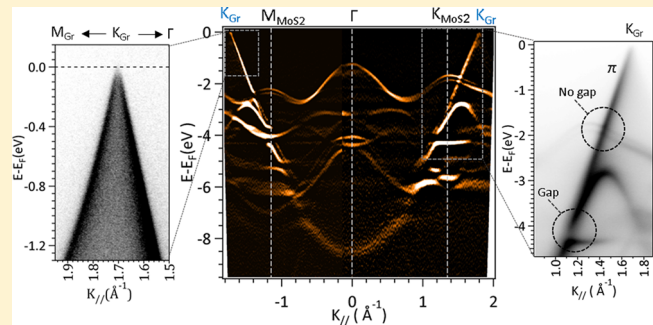
[†]Department of Physics, University of South Florida, Tampa, Florida 33620, United States

[‡]Synchrotron SOLEIL, L'Orme des Merisiers, Saint Aubin-BP 48, 91192 Gif sur Yvette Cedex, France

Supporting Information

ABSTRACT: Artificial heterostructures assembled from van der Waals materials promise to combine materials without the traditional restrictions in heterostructure-growth such as lattice matching conditions and atom interdiffusion. Simple stacking of van der Waals materials with diverse properties would thus enable the fabrication of novel materials or device structures with atomically precise interfaces. Because covalent bonding in these layered materials is limited to molecular planes and the interaction between planes are very weak, only small changes in the electronic structure are expected by stacking these materials on top of each other. Here we prepare interfaces between CVD-grown graphene and MoS₂ and report the direct measurement of the electronic structure of such a van der Waals heterostructure by angle-resolved photoemission spectroscopy. While the Dirac cone of graphene remains intact and no significant charge transfer doping is detected, we observe formation of band gaps in the π -band of graphene, away from the Fermi-level, due to hybridization with states from the MoS₂ substrate.

KEYWORDS: Graphene, heterostructures, van der Waals materials, ARPES, CVD-graphene



Artificial van der Waals heterostructures promise to combine materials with diverse properties by mechanical stacking^{1–3} or conventional growth^{4–6} of molecular heterolayers. This enables fabrication of novel materials or device structures with atomically precise interfaces.^{7–13} Because covalent bonding in these layered materials is limited to molecular planes, interface interactions between dissimilar materials are expected to modify the properties of the individual constituent layers only weakly.⁶ Here we present a nanoangle-resolved photoemission spectroscopy (nano-ARPES) study of the electronic structure of the graphene/MoS₂ interfaces. We show that the coveted gapless and undoped relativistic Dirac-cone for supported graphene is achieved at the Fermi-level, while in regions where the graphene π -band overlaps with out-of plane MoS₂ orbitals the opening of several band-gaps in the π -band is observed. This shows that the band structure of graphene and potentially other 2D materials can be efficiently tuned in van der Waals heterostructures.

The influence of interlayer interaction in transition metal dichalcogenides (TMDCs) has been extensively discussed since the discovery that their band structure changes^{14–16} for single layers compared to multilayer or bulk materials.^{17,18} Thus, not surprisingly there is increasing interest in such interlayer interactions for heterostructures^{3,6,19} as well. Although there has been some evidence of optical coupling in TMDCs heterostructures,³ no direct measurement that would demonstrate a change of the electronic structure due to interlayer

interaction in van der Waals heterostructures have been reported. In particular, to the best of our knowledge interfaces of graphene with a TMDCs have only once before been analyzed by angle-resolved photoemission electron spectroscopy (ARPES).²⁰ In contrast to the measurement reported here, the previous ARPES study of MoSe₂ grown on bilayer graphene on SiC did not observe a modification of the π -band of graphene due to interaction with the TMDC. This apparent discrepancy may be due to the limited k -space reported in the previous study or because of the different sample preparation. Here we investigate graphene transferred on top of a TMDC. To date, the utilization of momentum-space probe like ARPES has been hindered by the ability to prepare clean interfaces between polycrystalline CVD-grown graphene and TMDCs. On the other hand, reports on the potential applications of van der Waals heterostructures, including the graphene/MoS₂ interface, for example, in field effect transistor devices^{7,8,21} or for energy harvesting materials,^{22–24} become more frequent, demonstrating the practical potential for such heterostructures and consequently the need for better understanding of their interface electronic properties. Here, we utilize recently developed high-spatial resolution ARPES (or nanoARPES)²⁵ capable of combining multi- and single-grain imaging using

Received: October 30, 2014

Revised: December 29, 2014

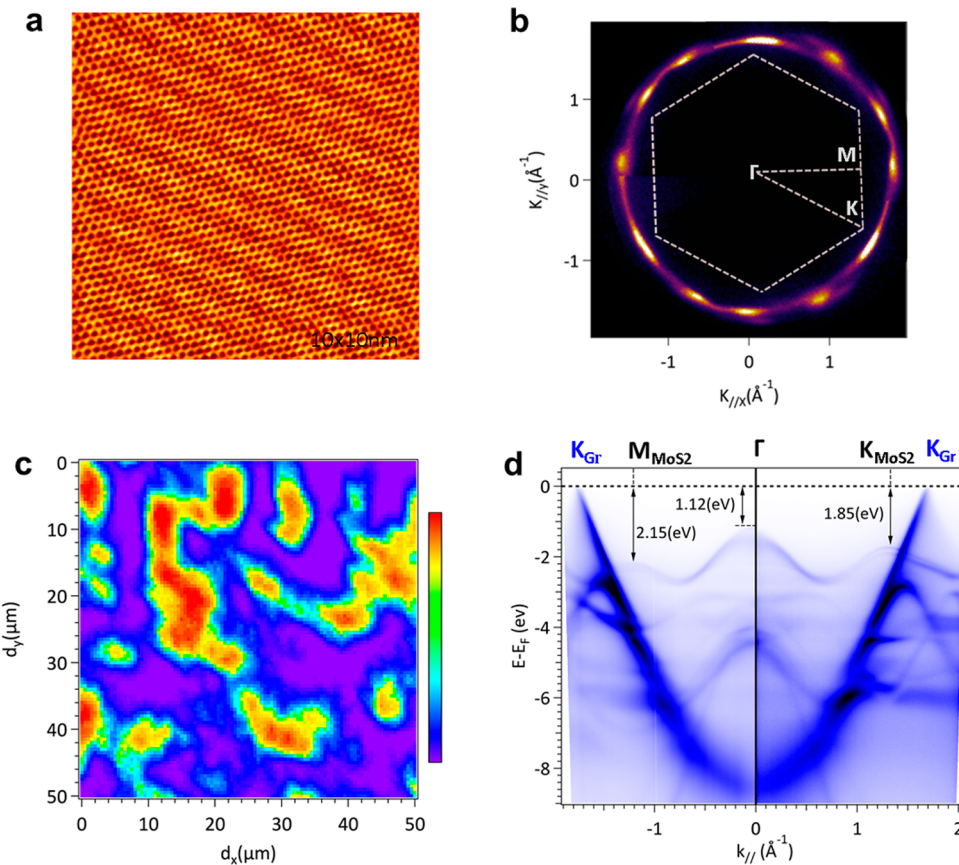


Figure 1. Structure of transferred CVD-grown graphene. (a) High-resolution STM image of ultraflat graphene transferred to MoS₂ ($I_t = 33$ nA and $V_{\text{bias}} = -50$ mV). Only a weak moiré structure superimposed on the atomic honeycomb structure of graphene is observed. (b) Fermi surface map measured by ARPES with 100 eV p-polarized light at room temperature of the polycrystalline graphene. The observed intensity variation along the “Fermi surface ring” is a consequence inhomogeneity of the graphene grain distribution within the sampling area. The orientation of the substrate MoS₂ BZ is also indicated. (c) Nano-ARPES microscopy image of specific grain orientations indicating grains of 5–10 μm in size. (d) ARPES E - k spectrum along the M- Γ -K direction of the MoS₂ BZ with the π - and σ -bands of the polycrystalline graphene superimposed. The valence band maximum of MoS₂ at the Γ -point is measured at 1.12 eV below the Fermi-level.

synchrotron radiation. This enables us to measure the low-energy electronic dynamics down to individual pristine graphene grains in contact with MoS₂ surfaces and thus to shed light on fundamental features like doping, gap-size, Fermi velocity, and interface hybridization in graphene/MoS₂ heterostructures.

In our studies, polycrystalline CVD-grown graphene has been transferred to freshly air-cleaved MoS₂ substrates.²⁶ A description of the sample preparation and characterization may be found in the Supporting Information. Atomically resolved scanning tunneling microscopy images, shown in Figure 1, demonstrate the cleanliness (see also C-1s spectrum in Supporting Information Figure S1) and ultraflat surface of graphene supported on MoS₂ with only a weak moiré-structure visible at very high tunneling currents. This faint moiré-structure indicates that the MoS₂ only induces a weak superpotential on graphene, in contrast to the case of graphene on hex-BN.²⁷ On these samples both ARPES and nanoARPES measurements have been performed, with a photon-beam spot size of $\sim 200 \mu\text{m}$ and ~ 120 nm, respectively. Figure 1 d show the classical ARPES band structure along (M- Γ -K)_{MoS₂} symmetry directions of the graphene covered MoS₂ single crystal. Well-defined graphene-derived σ - and π -dispersing bands are observed due to emission from graphene grains that are coincidentally aligned with the substrate. The valence band

maximum of MoS₂ at the Γ -point is measured at 1.12 eV with respect to the Fermi-level. Taking the bulk band gap of MoS₂ as 1.23–1.3 eV (depending on reported literature values) we see that there is ~ 0.09 –0.18 eV barrier for electron injection from graphene to MoS₂. This is a small barrier but not quite the close-to barrierless contact between graphene and multilayer MoS₂ as suggested from some device characterization.^{7,8}

At the Fermi-level MoS₂ possess no states and consequently the Fermi-surface of the interface is governed by the graphene-states at the Dirac-point. Because of the polycrystalline nature of the samples and the large photon spot size in conventional ARPES, we observe a circular Fermi-surface with a vector radius of $k_{\parallel} = 1.703 \text{ \AA}^{-1}$, as shown in Figure 1 b. This “Fermi-surface” is the superpositioning of all the K-points of the graphene grains within the photon beam. NanoARPES, on the other hand, enables to focus the photon beam on a single graphene grain. By collecting photoelectrons emitted from a given energy and momentum, for example, the Fermi-level at the K-point of a specific graphene orientation, and raster-scanning the sample, one can obtain real space image that provides the location, shape, and orientation of graphene grains. Figure 1c shows such an image for a specific graphene-grain orientation. In this way graphene-grains can be selected for detailed band structure measurements. Our microscopic imaging of the graphene reveals that our sample is made of anisotropically oriented \sim –

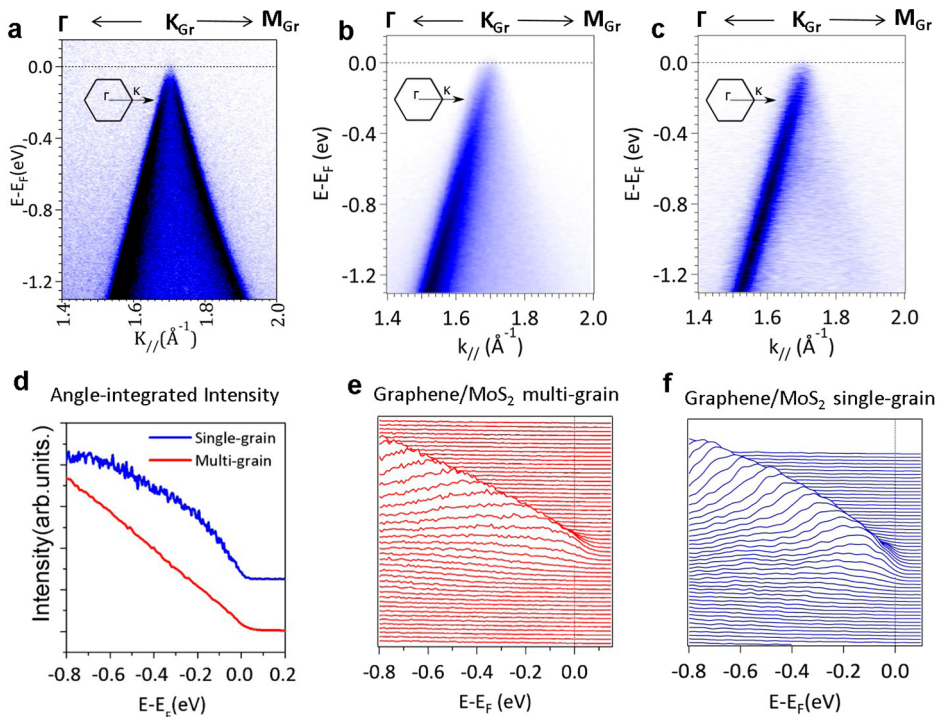


Figure 2. Structure of the Dirac cone for graphene on MoS₂. (a,b) ARPES near the Fermi level using 30 eV circular polarized light and 100 eV p-polarized light, respectively along the $\Gamma_{(1)}\text{-K}\text{-M}_{(2)}$ direction. Because ARPES is measured on polycrystalline graphene the Dirac-cone envelop is “filled” from photoemission of randomly aligned graphene grains. (c) Nano-ARPES of a single graphene grain using 100 eV p-polarized light at 77K. Both ARPES and nano-ARPES show a perfect Dirac cone with the Fermi-level at the Dirac-point. (d) Angle-integrated photoemission intensity as a function of binding energy for ARPES and nano-ARPES, that is, multi- and single-graphene-grains. In both cases, the intensity drops to zero directly at the Fermi-level indicating that the Dirac-point lies at the Fermi-level and no doping or band gap opening is observed. The energy distribution curves for ARPES and nano-ARPES are shown in (e,f), respectively.

10 μm long pristine single crystal graphene grains with random orientation with respect to the MoS₂ surface.

Figure 2 shows a close inspection of the Dirac cone for multi-(ARPES) and single- (nanoARPES) graphene grains. Figure 2a shows an ARPES spectrum taken with circular polarized light of $h\nu = 30$ eV across the K-point of an arbitrary grain along the $\Gamma_{(1)}\text{-K}\text{-M}_{(2)}$ direction of graphene. Because of the simultaneous measurement of many graphene-grain orientations in ARPES the spectrum displays a “filled Dirac cone” where the photoemission intensity within the Dirac cone-envelop is due to randomly oriented grains. A similarly broadened cone is observed with p-polarized light of $h\nu = 100$ eV, shown in Figure 2b. However, under these conditions only one branch of the Dirac-cone can be observed because of photoemission selection rules.²⁵ NanoARPES provides a more detailed look at the π -band of an individual graphene domain. Figure 2c shows nanoARPES data of the π -band close to the Fermi-level in the $\Gamma\text{-K}$ direction. From the known K-point position it can be determined that the Dirac cone intersects with the Fermi-level directly at the K-point. This is further demonstrated by angle integrated photoemission intensity and energy distribution curves (EDC), displayed in Figure 2d–f. All these data show that the graphene on MoS₂ is undoped and exhibits no band gap at the Dirac-point. In an earlier study, we deduced a slight p-doping of graphene from C-1s core level analysis.²⁶ The measurement of the Dirac cone reported here is a direct method to determine the doping and thus much more accurate. One possible reason why the previous estimate was incorrect may be the use of the C-1s peak position for HOPG as a reference for charge neutral graphene, this may not be correct

and result in a systematic error. This needs, however, further investigation. From the ARPES measurements we also determine a Fermi-velocity of 1.03×10^6 m/s and the momentum distribution curve (MDC) (see Supporting Information Figure S2) is very narrow illustrating the excellent quality of the transferred graphene. Obtaining a perfect Dirac cone, like the one observed here, has been challenging for most supported graphene systems, as may be appreciated for the case of graphene on copper prior to the transfer to MoS₂ (see Supporting Information Figure S3). Thus, the MoS₂ substrate may be ideal for studies that require Dirac relativistic carriers in graphene. Furthermore, it is interesting to point out that for graphene/MoS₂ we do not observe any replica Dirac cones due to a substrate-induced superstructure (moiré-pattern) even for graphene grains closely aligned with the substrate. This is in agreement with the weak moiré pattern in the STM data and in contrast to graphene/hex-BN.²⁷

Differently to energies close to the Fermi-level, the π -band of graphene at higher binding energies is significantly altered by the interaction with the MoS₂ substrate. ARPES with $h\nu = 30$ eV light shows an opening of a band gap in the graphene’s π -band, as shown in Figure 3a. Additional ARPES measurements with $h\nu = 100$ eV are shown in Figure 3b,c. Along the $(\Gamma\text{-M})_{\text{MoS}2}$ and $(\Gamma\text{-K})_{\text{MoS}2}$ directions, four and three distinctive gaps are observed, respectively, labeled in sequential order. Calculated second derivatives of the $E\text{-k}$ spectra accentuate the gaps and this processed data can be found in the Supporting Information Figure S4b. The gaps are of significant size of up to $\sim 0.8 \pm 0.02$ eV and occur where certain MoS₂ bands intersect the graphene π -band. It is known from the layer-dependent

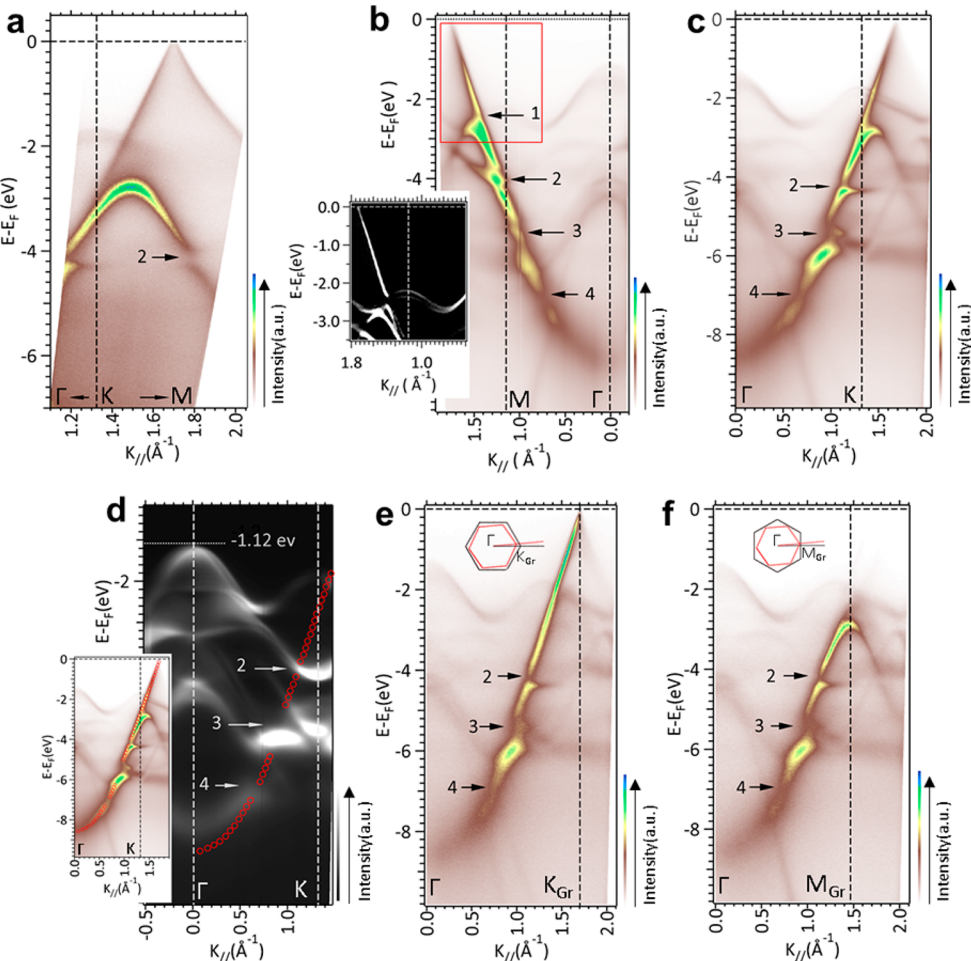


Figure 3. Modification of graphene π -band through hybridization with MoS₂ bands. (a) ARPES with 30 eV circular polarized light along the $(\Gamma\text{-}\text{M})_{\text{MoS}_2}$ direction. A band gap in the π -band is observed labeled “2”. More band gaps can be seen using p-polarized light with 100 eV photonenergy (b–f). ARPES data for graphene on MoS₂ along (b) $(\Gamma\text{-}\text{M})_{\text{MoS}_2}$ and (c) $(\Gamma\text{-}\text{K})_{\text{MoS}_2}$. Observed band gaps are labeled 1 through 4. The inset in (b) shows a zoom-in of the 2nd derivate of ARPES data, which allows better identification of band gap “1”. The 2nd derivatives of the entire spectra can be found in the Supporting Information. To illustrate the occurrences of band gaps due to band crossing with MoS₂ bands we show in (d) the bare MoS₂ substrate measured with p-polarized light, which accentuates out-of plane molecular orbitals. Superimposed on (d) is the experimental π -band (red circles) and its gaps extracted from the inset (same data as (c)). It is apparent that gaps occur in regions with strong photoemission intensity of the MoS₂ substrate, that is, in regions with out-of plane orbital character. Nano-ARPES for two $\sim 30^\circ$ rotated graphene grains along their $(\Gamma\text{-}\text{K})_{\text{graphene}}$ and $(\Gamma\text{-}\text{M})_{\text{graphene}}$ directions is shown in (e) and (f), respectively. Because of the graphene grain rotation both these nano-ARPES measurements are taken along almost the same MoS₂ substrate direction. The directions for the nano-ARPES measurements with respect to MoS₂-substrate and graphene for the two grains are schematically illustrated in the inset. Despite the different azimuth direction of graphene the band gaps occur at the same binding energy, further illustrating that they are a consequence of the MoS₂ band structure.

electronic properties of pure MoS₂ that it is the bands with out-of plane orbital character that are responsible for interlayer interaction and modification of the electronic structure for multilayers versus monolayer.^{17,18} Thus, for the graphene/MoS₂ heterosystem it seems similarly plausible that the bands with out-of plane orbital character of the MoS₂ cause hybridization with the graphene π -band if they overlap in energy and k-vector. To demonstrate this experimentally, we took ARPES spectra of a bare MoS₂ substrate with p-polarized light, which emphasizes bands with surface-normal orbitals. In Figure 3d, we superimpose the measured graphene π -band with its gaps on the measured bare MoS₂ band structure. It is apparent that the gaps indeed occur in regions with the strongest photoemission intensity, that is, strong out-of-plane character, while where the intensity is weak, for example, for the valence band maximum close to the MoS₂ K-point, no gaps in the graphene π -band are induced. To obtain a more

quantitative assignment of the MoS₂ orbitals we compare our measurements with previously reported theoretical band structure calculations, reproduced in the Supporting Information Figure S4a, of the bare MoS₂ surface.²⁸ Table 1 summarizes the size of the observed band gaps and the orbital character of the MoS₂ substrate that induces them. Noticeably, because of the orbital character of the valence band maximum of graphene along different directions of its BZ the gap labeled as “1” can only be seen along the $(\Gamma\text{-}\text{M})_{\text{MoS}_2}$ direction, while it is absent in the $(\Gamma\text{-}\text{K})_{\text{MoS}_2}$ direction (see Supporting Information Figure S5 and S6 for detailed ARPES-data around these two k-space regions). In the latter direction, the MoS₂ band at the valence band maximum has predominantly in-plane character in agreement with the above-discussed p-polarized photoemission data for bare MoS₂.

Finally, by performing nano-ARPES, shown in Figure 3e,f, we are able to verify that the electronic interaction between

Table 1. Summary of Band Gaps (Measured from EDC of ARPES Data, Shown in the Supporting Information) in the π -Band of Graphene and the Molecular Orbitals of MoS₂ Responsible for the Band Gap Opening

gap no. according to Figure S4b	midgap binding energy [eV]	gap- size [eV]	points in MoS ₂ BZ	MoS ₂ -out of plane orbitals, from ref 28
1	~2.39	0.3	roughly $\pm 15^\circ$ from M _{MoS₂} -point	Mo: d z ²
2	~3.96	0.74	All directions	S: p z
3	~5.51	0.77	All directions	S: p z and/or Mo: d z ²
4	~6.94	0.57	All directions	Mo: d z ²

graphene and MoS₂ is independent of the stacking register of the two heterolayers. NanoARPES spectra of two single graphene grains, one with its $(\Gamma\text{-}K)$ _{graphene} and the other with its $(\Gamma\text{-}M)$ _{graphene} direction closely aligned (within $\pm 1.5^\circ$) with the same $(\Gamma\text{-}K)$ _{MoS₂} direction, show that band gaps "2", "3", and "4" occur at precisely the same binding energies. This demonstrates that the opening of the band gaps is determined by the band structure of MoS₂ and the specific rotation of the graphene grain does not significantly affect the band gaps.

In conclusion, the opening of band gaps in graphene supported on TMDCs, and likely on other van-der Waals materials, can be easily predicted from the out-of-plane orbital components in the TMDC band structure. The large family of 2D-materials with diverse properties allows a flexible approach for creating band gaps in the graphene π -band by choosing appropriate substrates and thus provides an approach for tuning, for example, optical transitions in graphene.

We also mention that the hybridization of graphene π -states with surface normal orbitals is not without precedence. For graphene on weakly interacting metals such as Ag²⁹ and Au,³⁰ the π -band remains intact with the exception of small band-gaps where the metal d-bands cross the π -band. Interestingly, in the case of heavy elements like Au the hybridization of the metal orbitals with graphene also induces a spin-polarization of graphene at the Fermi-level.³⁰ The investigation of spin polarization of graphene by supporting it on TMDCs containing heavy elements, like, for example, WS₂, thus may be an exciting future direction for creating a robust spin-polarization in graphene with an intact Dirac cone and supported on a semiconducting substrate.

ASSOCIATED CONTENT

Supporting Information

Sample preparation and characterization methods; C-1s soft XPS spectrum; momentum distribution curve (MDC) of π -band close to Fermi-level; comparison of Dirac cone for graphene on Cu and transferred graphene to MoS₂; comparison of measured band structure with calculated structure for MoS₂; ARPES data for graphene π -band intersecting with the VBM-band of MoS₂, that is, orientation-dependent opening of gaps; EDCs across gaps in the π -band for estimation of band gap values. This material is available free of charge via the Internet at <http://pubs.acs.org>.

AUTHOR INFORMATION

Corresponding Author

*E-mail: mbatzill@usf.edu.

Notes

The authors declare no competing financial interest.

ACKNOWLEDGMENTS

The USF group acknowledges financial support from NSF-DMR under Grant 1204924. M.B. also acknowledges support from the Technische Universität München-Institute for Advanced Study, funded by the German Excellence Initiative and the European Union Seventh Framework Programme under Grant 291763.

REFERENCES

- Geim, A. K.; Grigorieva, I. V. Van der Waals heterostructures. *Nature* **2013**, *449*, 419–425.
- Gao, G. H.; Gao, W.; Cannuccia, E.; Taha-Tijerina, J.; Balicas, L.; Mathkar, A.; Narayanan, T. N.; Liu, Z.; Gupta, B. K.; Peng, J.; Yin, Y. S.; Rubio, A.; Ajayan, P. M. Artificially Stacked Atomic Layers: Towards New van der Waals Solids. *Nano Lett.* **2012**, *12*, 3518–3525.
- Fang, H.; Battaglia, C.; Carraro, C.; Nemsak, S.; Ozdol, B.; Kang, J. S.; Bechtel, H. A.; Desai, S. B.; Kronast, F.; Unal, A. A.; Conti, G.; Conlon, C.; Palsson, G. K.; Martin, M. C.; Minor, A. M.; Fadley, C. S.; Yablonovitch, E.; Maboudian, R.; Javey, A. Strong interlayer coupling in van der Waals heterostructures built from single-layer chalcogenides. *Proc. Natl. Acad. Sci. U.S.A.* **2014**, *111*, 6198–6202.
- Lin, Y.-C.; Lu, N.; Perea-Lopez, N.; Li, J.; Lin, Z.; Peng, X.; Lee, C. H.; Sun, C.; Calderin, L.; Browning, P. N.; Bresnahan, M. S.; Kim, M. J.; Mayer, T. S.; Terrones, M.; Robinson, J. A. Direct Synthesis of van der Waals Solids. *ACS Nano* **2014**, *8*, 3715–3723.
- Addou, R.; Dahal, A.; Batzill, M. Growth of a two-dimensional dielectric monolayer on quasi-freestanding graphene. *Nat. Nanotechnol.* **2013**, *8*, 41–45.
- Alidoust, N.; Bian, G.; Xu, S. Y.; Sankar, R.; Neupane, M.; Liu, C.; Belopolski, I.; Qu, D. X.; Denlinger, J. D.; Chou, F. C.; Hasan, M. Z. Observation of monolayer valence band spin-orbit effect and induced quantum well states in MoX₂. *Nat. Commun.* **2014**, *5*, 4673.
- Yoon, J.; Park, W.; Bae, G.-Y.; Kim, Y.; Jang, H. S.; Hyun, Y.; Lim, S. K.; Kahng, Y. H.; Hong, W.-K.; Lee, B. H.; Ko, H. C. Highly flexible and transparent multilayer MoS₂ transistors with graphene electrodes. *Small* **2013**, *9*, 3295–3300.
- Roy, T.; Tosun, M.; Kang, J. S.; Sachid, A. B.; Desai, S. B.; Hettick, M.; Hu, C. C.; Javey, A. Field-Effect Transistors Built from All Two-Dimensional Material Components. *ACS Nano* **2014**, *8*, 6259–6264.
- Dean, C. R.; Young, A. F.; Meric, I.; Lee, C.; Wang, L.; Sorgenfrei, S.; Watanabe, K.; Taniguchi, T.; Kim, P.; Shepard, K. L.; Hone, J. Boron nitride substrates for high-quality graphene electronics. *Nat. Nanotechnol.* **2010**, *5*, 722–726.
- Britnell, L.; Gorbachev, R. V.; Jalil, R.; Belle, B. D.; Schedin, F.; Mishchenko, A.; Georgiou, T.; Katsnelson, M. I.; Eaves, L.; Morozov, S. V.; Peres, N. M. R.; Leist, J.; Geim, A. K.; Novoselov, K. S.; Ponomarenko, L. A. Field-Effect Tunneling Transistor Based on Vertical Graphene Heterostructures. *Science* **2012**, *335*, 947–950.
- Choi, M. S.; Lee, G.-H.; Yu, Y.-J.; Lee, D.-Y.; Lee, S. H.; Kim, P.; Hone, J.; Yoo, W. J. Controlled charge trapping by molybdenum disulphide and graphene in ultrathin heterostructured memory devices. *Nat. Commun.* **2013**, *4*, 1624.
- Hong, X.; Kim, J.; Shi, S.-F.; Zhang, Y.; Jin, C.; Sun, Y.; Tongay, S.; Wu, J.; Zhang, Y.; Wang, F. Ultrafast charge transfer in atomically thin MoS₂/WS₂ heterostructures. *Nat. Nanotechnol.* **2014**, *9*, 682–686.
- Dean, C. R.; Wang, L.; Maher, P.; Forsythe, C.; Ghahari, F.; Gao, Y.; Katoch, J.; Ishigami, M.; Moon, P.; Koshino, M.; Taniguchi, T.; Watanabe, K.; Shepard, K. L.; Hone, J.; Kim, P. Hofstadter's butterfly and the fractal quantum Hall effect in moiré superlattices. *Nature* **2013**, *497*, 598–602.
- Mak, K. F.; Lee, C.; Hone, J.; Shan, J.; Heinz, T. F. Atomically thin MoS₂: A new direct-gap semiconductor. *Phys. Rev. Lett.* **2010**, *105*, 136805.

- (15) Splendiani, A.; Sun, L.; Zhang, Y.; Li, T.; Kim, J.; Chim, C.-Y.; Galli, G.; Wang, F. Emerging Photoluminescence in Monolayer MoS₂. *Nano Lett.* **2010**, *10*, 1271–1275.
- (16) Wencan, J.; Yeh, P. C.; Zaki, N.; Zhang, D.; Sadowski, J. T.; Al-Mahboob, A.; van der Zande, A. M.; Chenet, D. A.; Dadap, J. I.; Herman, I. P.; Sutter, P.; Hone, J.; Osgood, R. M., Jr. Direct measurement of the thickness-dependent electronic band structure of MoS₂ using angle resolved photoemission spectroscopy. *Phys. Rev. Lett.* **2013**, *111*, 106801.
- (17) Lebègue, S.; Eriksson, O. Electronic structure of two-dimensional crystals from ab initio theory. *Phys. Rev. B* **2009**, *79*, 115409.
- (18) Kuc, A.; Zibouche, N.; Heine, T. Influence of quantum confinement on the electronic structure of the transition metal sulfide TS₂. *Phys. Rev. B* **2011**, *83*, 245213.
- (19) Li, X. D.; Yu, S.; Wu, S. Q.; Wen, Y. H.; Zhou, S.; Zhu, Z. Z. Structural and Electronic Properties of Superlattice Composed of Graphene and Monolayer MoS₂. *J. Phys. Chem. C* **2013**, *117*, 15347–15353.
- (20) Zhang, Y.; Chang, T.-R.; Zhou, B.; Cui, Y. T.; Yan, H.; Liu, Z.; Schmitt, F.; Lee, J.; Moore, R.; Chen, Y.; Lin, H.; Jeng, H. T.; Mo, S. K.; Hussain, Z.; Bansil, A.; Shen, Z. X. Direct observation of the transition from indirect to direct bandgap in atomically thin epitaxial MoSe₂. *Nat. Nanotechnol.* **2014**, *9*, 111–115.
- (21) Shih, C.-J.; Wang, Q. H.; Son, Y.; Jin, Z.; Blankschtein, D.; Strano, M. S. Tuning On–Off Current Ratio and Field-Effect Mobility in a MoS₂–Graphene Heterostructure via Schottky Barrier Modulation. *ACS Nano* **2014**, *8*, 5790–5798.
- (22) Wi, S.; Chen, M.; Nam, H.; Liu, A. C.; Meyhofer, E.; Liang, X. High blue-near ultraviolet photodiode response of vertically stacked graphene-MoS₂-metal heterostructures. *Appl. Phys. Lett.* **2014**, *104*, 232103.
- (23) Zhang, W.; Chuu, C.-P.; Huang, J.-K.; Chen, C.-H.; Tsai, M.-L.; Chang, Y.-H.; Liang, C.-T.; He, H., Jr.; Chou, M.-Y.; Li, L.-J. Ultrahigh-Gain Phototransistors Based on Graphene-MoS₂ Heterostructures. *Sci. Rep.* **2014**, *4*, 3826.
- (24) Britnell, L.; Ribeiro, R. M.; Eckmann, A.; Jalil, R.; Belle, B. D.; Mishchenko, A.; Kim, Y.-J.; Gorbachev, R. V.; Georgiou, T.; Morozov, S. V.; Grigorenko, A. N.; Geim, A. K.; Casiraghi, C.; Castro Neto, A. H.; Novoselov, K. S. Strong Light-Matter Interactions in Heterostructures of Atomically Thin Films. *Science* **2013**, *340*, 1311–1314.
- (25) Avila, J.; Razado, I.; Lorcy, S.; Fleurier, R.; Pichonat, E.; Vignaud, D.; Wallart, X.; Asensio, M. C. Exploring electronic structure of one-atom thick polycrystalline graphene films: A nano angle resolved photoemission study. *Sci. Rep.* **2013**, *3*, 2439.
- (26) Coy-Diaz, H.; Addou, R.; Batzill, M. Interface properties of CVD grown graphene transferred onto MoS₂(0001). *Nanoscale* **2014**, *6*, 1071–1078.
- (27) Yankowitz, M.; Xue, J.; Cormode, D.; Sanchez-Yamagishi, J. D.; Watanabe, K.; Taniguchi, T.; Jarillo-Herrero, P.; Jacquod, P.; LeRoy, B. J. Emergence of superlattice Dirac points in graphene on hexagonal boron nitride. *Nat. Phys.* **2012**, *8*, 382–386.
- (28) Han, S. W.; Cha, G.-B.; Frantzeskakis, E.; Razado-Colombo, I.; Avila, J.; Park, Y. S.; Kim, D.; Hwang, J.; Kang, J. S.; Ryu, S.; Yu, W. S.; Hong, S. C.; Asensio, M. C. Band-gap expansion in the surface-localized electronic structure of MoS₂ (0002). *Phys. Rev. B* **2012**, *86*, 115105.
- (29) Papagno, M.; Moras, P.; Sheverdyeva, P. M. Doppler, J., Garhofer, A., Mittendorfer, F., Redinger, J., Carbone, C. Hybridization of graphene and a Ag monolayer supported on Re(0001). *Phys. Rev. B* **2013**, *88*, 235430.
- (30) Shikin, A. M.; Rybkin, A. G.; Marchenko, D.; Rybkina, A. A.; Scholz, M. R.; Rader, O.; Varykhlov, A. Induced spin-orbit splitting in graphene: the role of atomic number of the intercalated metal and π -d hybridization. *New J. Phys.* **2013**, *15*, 013016.